Chapter 4

Pulsed Laser Deposition of ITO: From Films to Nanostructures

Seong Shan Yap, Thian Khok Yong,
Chen Hon Nee and Teck Yong Tou

Additional information is available at the end of the chapter

http://dx.doi.org/10.5772/65897

Abstract

Indium-tin oxide (ITO) films have been deposited by pulsed laser deposition (PLD) to achieve low resistivity and high transmittance in visible region. Important parameters governing the growth of ITO films, which include laser wavelength, substrate temperature, and the background gas pressure, are discussed. By utilizing the energetic plasma in laser ablation of an ITO target, relatively low substrate temperature growth has been demonstrated. Room temperature deposition enables ITO films to be deposited on the polymer substrate. In addition, deposition in different background gases promotes the catalyst-free growth of nanostructured ITO films. In particular, deposition in Ar or He at optimized pressures enables the growth of highly crystalline ITO nanostructures, which include nanorods and nanowires due to the self-catalyzed growth from the plasma plume. The conditions which allow the pulsed laser deposition of ITO thin films and the growth of nanostructured ITO are reviewed and discussed.

Keywords: pulsed laser deposition, ITO, nanostructures, nanowires, nanorods, TCO

1. Introduction

Sn-doped indium oxide or indium tin oxide (ITO) plays important roles in optoelectronics applications by providing contact layer with high transparency in the visible. Currently, ITO remains as the transparent conducting oxide (TCO) with the lowest resistivity on a commercial scale (1–2 × 10^{-4} Ω cm) [1]. In order to obtain both conductivity and transparency, the carrier density should not be too high to maintain its transparency with sufficiently low resistivity/sheet resistance. In addition, the carrier mobility can be maximized, which will then provide active carriers for conduction. **Figure 1** shows the band structure of the undoped In_2O_3 and

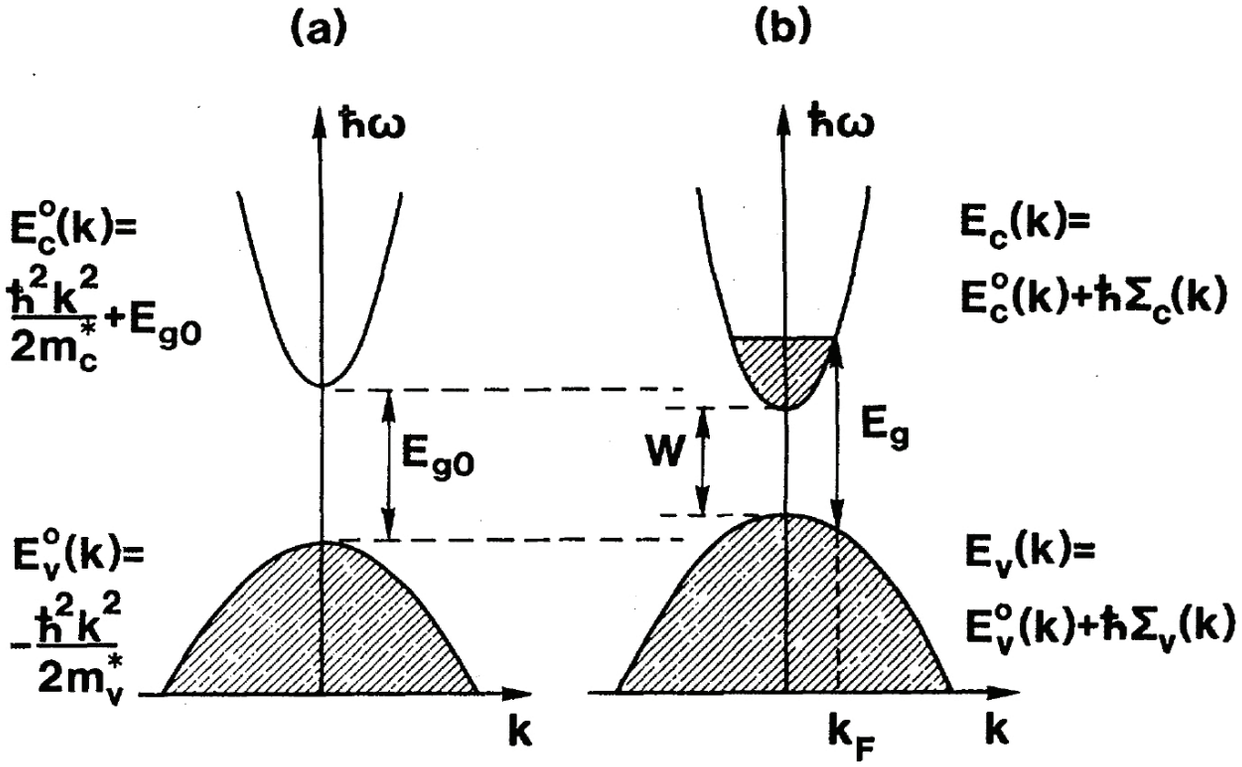

Figure 1. Schematic illustration of the assumed parabolic band structure of (a) undoped and (b) heavily Sn-doped In_2O_3 in the vicinity of the top of the valence band and the bottom of the conduction band with a band gap E_{go}. A vertical shift in the conduction and valence bands is apparent after heavy Sn doping in (b) assumed to have the sole effect of widening the band gap by a Burstein-Moss shift W due to filling up of the lowest states in the conduction band. Shaded areas denote occupied states. Band gaps, Fermi wave number k_F, and dispersion relations are indicated [2].

heavily Sn-doped In_2O_3 that was proposed by Hamberg et al. [2]. The band structure for In_2O_3 has a parabolic band that is characterized by effective mass m_c^* for the conduction band and m_v^* for the valence band. The direct band gap (E_{go}) is around 3.75 eV. After optimized Sn doping, the band gap (E_g), the carrier density, and mobility are increased, giving rise to the increase in carriers for conduction while maintaining the transparency. The change in carrier density, defect states, and crystallinity thus affects the final quality of the films.

ITO films can be grown by various methods. **Table 1** gives an overview of the requirements and performance of the different deposition techniques assessed against various different fundamental criteria. The deposition conditions of ITO crucially affect the dopant density, crystallinity, nanostructures formation, and defects in the films. Some of the common thin film deposition techniques are thermal evaporation, sputtering, pulsed laser deposition (PLD), chemical vapor deposition (CVD), and atomic layer deposition (ALD) which are becoming popular in recent years. These techniques can be broadly compared in terms of the energy of depositing specie, substrate temperature and possibly the annealing process after the film is deposited, and some specific features of the techniques.

The energy of depositing species, or the kinetic energy, is determined by the method for vapor creation. For TE, CVD, and ALD, the vapor is largely created via heating effect, which involves thermalization among the vapor species. Generally, a thermalized vapor is

	Thermal evaporation (TE)	Chemical vapor deposition (CVD)	Atomic layer deposition (ALD)	Sputtering (S)	Pulsed laser deposition (PLD)
Depositing species	Atoms/ions	Precursors molecules	Precursors molecules	Atoms/ions	Atoms/ion/clusters
Energy of depositing species	Low (0.1–0.5 eV)	Low	Low	Normally low, 1–100 eV (with biasing)	Low to very high 1–1000 eV
Substrate temperature	None	Typically high	Varies with precursor	Low to moderate	Low to moderate
Features	High growth rate, simple	Continuous growth	Step growth-layer by layer, scalable	Nonreactive and reactive deposition DC or RF sputtering	Nonreactive and reactive deposition, suitable for stoichiometric films, large control range for different dopants

Table 1. Different deposition techniques.

ideal for better control of the thin film morphology and microstructures; hence, a uniform thin film or coating is always achieved. The TE method remains one of the popular choices for metallic thin film deposition, such as the metal contact or electrodes. The disadvantage of TE method is always the contaminations due to out-diffusion from the walls of deposition chamber as a result of high temperature required to vaporize the targets. To reduce these contaminations, thin film deposition by TE always necessitates high vacuum condition, typically 10^{-4} Pa or better. On the other hand, CVD is operated at relatively lower temperatures, owing to dissociation energy of the precursors, but requires high substrate heating. As the precursors are constantly supplied from external sources, the film growth is a continuous process, easily multi-element control, good stoichiometry, and epitaxial. The precursors are usually volatile and/or toxic in gaseous state, and thus, the requirement for safety and environmental contamination is important. To obtain high quality and purity of the epitaxial thin films, the high vacuum requirement of CVD is usually more stringent than that for TE.

For deposition of metal oxide–based thin films, however, TE is generally not used due to refractory high temperature for vaporization from solid targets. However, the CVD methods are usually applicable for metal oxide thin film deposition from the metal organic precursors at relatively low temperature of about 200°C. In this respect, the ALD method has gained high popularity for ultrathin oxide deposition for encapsulation of devices against moisture and oxygen contaminations in recent years. With advent of nanoscale devices, which demand higher degrees of accuracy and control in terms of conformity and film thickness at Angstrom level, ALD has superseded the capability of CVD. In addition, ALD has established to be a better method for film composition for a wide range of materials, which include metals, semiconductor, and insulators of both crystalline and amorphous phase for different electronic applications in industries and manufacturing. However, for car industry and energy-efficiency buildings, smart windows with photocatalytic functions are proposed, which require not just cost-effective but also high throughput of coating method. Thus, the

atmospheric pressure CVD or APCVD method is applied for transition metal oxide thin film deposition.

PLD [3] and sputtering are considered more "versatile" methods for normal thin film deposition mainly because they employ direct vaporization to produce the required deposition flux. In particular, PLD has attracted much interest mainly due to its ability to deposit of high T_c superconducting films with necessary stoichiometry. While PLD can be operated between high vacuum and low pressure, the sputtering method is usually operated at low pressures with a continuous gas flow. For both methods, the production of a wide range of kinetic energy for the depositing specie ensures thin film depositions from different types of solid targets including doped target such as ITO. The film stoichiometry or multicomponent control is often obtained with the use of background gases for moderation of kinetic energy. While a suitable energy range can facilitate the growth of more uniform and crystalline thin films, the presence of background gas often prevents the film damage by energetic ion bombardment. For PLD, the background gases at suitable pressures may also introduce gas-phase reactions which may generate new species and/or formation of nanoclusters prior to the deposition on the substrate.

2. Pulsed laser deposition of ITO films

A typical experimental setup of PLD is shown in **Figure 2** [4] where ablation can be obtained by laser with different wavelengths or pulse duration, in either background gas or vacuum. Deposition of ITO is normally performed in O_2 environment to preserve the stoichiometry, similar to the deposition of superconducting oxide. In addition, the substrates can be heated

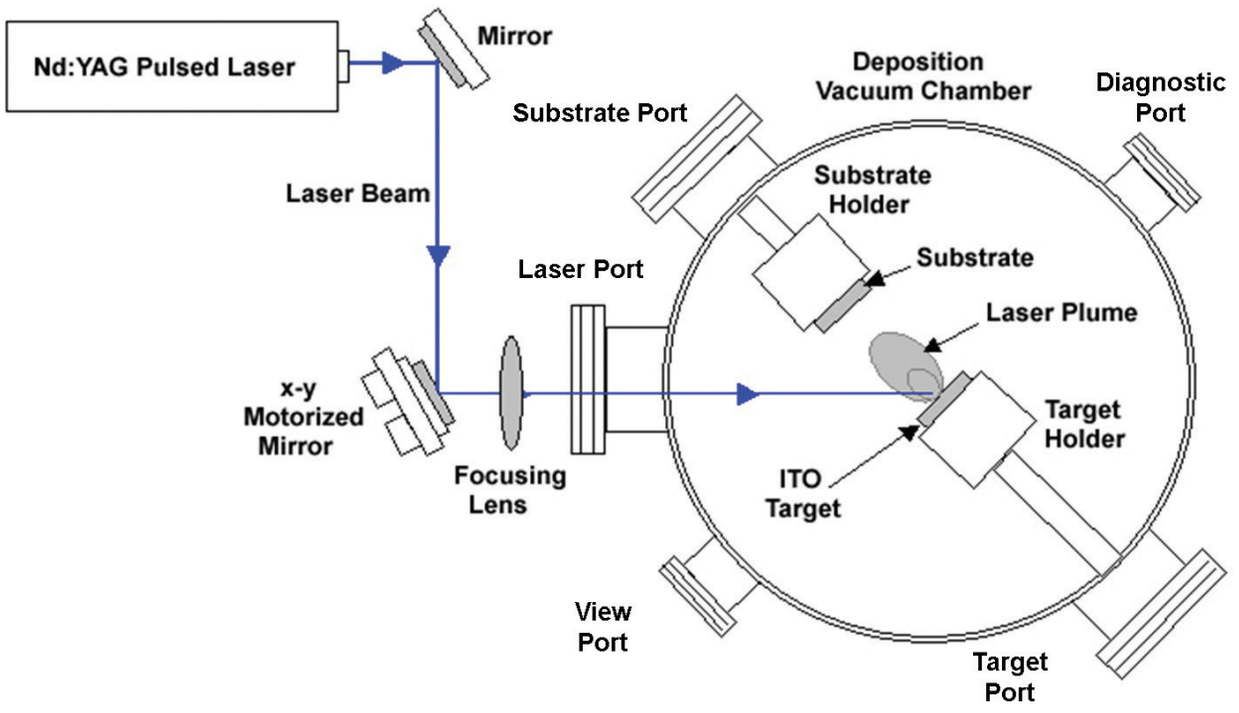

Figure 2. PLD setup for ITO growth. Deposition is often carried out in O_2 background.

References	Substrate	ITO (wt.% of SnO_2)	Lowest resistivity ($\times 10^{-4}$ Ω cm)	Optical transmittance	P_{O2} (mTorr)	d_{TS} (cm)	t (nm)	Laser parameters
[12, 13]	Glass	5	RT: 4 300°C: 2	RT: ~85% 300°C: ~92%	10	4.7	RT: 150 300°C: 170	Pulsed duration = 30 ns; Repetition rate = 10 Hz; Fluence ~2 J/cm²
[14]	PET	5	RT: 7 100°C: 4.1	RT: ~87% 100°C: ~90%	40	5.8	200	
[15]	Glass	10	RT: 5.35 200°C: 1.75	>85%	10	7	100	
[16]	Fused-Quartz	5	RT: 4.76	>90%	10	7	100 ± 20	
[16]	Fused-Quartz	10	RT: 5.56	>90%	10	7	100 ± 20	
[17]	PC	5	RT: 2.5	NA	9.75	7	100	
[18]	Glass	NA	RT: 5	>90%	10	10.5	NA	Repetition rate = 5 Hz; Fluence ~2 J/cm² *UV assisted
[19]	Glass	10	RT: 4	~88%	10	3.45	400	Repetition rate = 10 Hz; Fluence ~2 J/cm² *N_2
[20]	Quartz	10	RT: 5 300°C: 2.5	88%	10	NA	180	Fluence ~2 J/cm²
[21]	Glass	5	RT: 5.5 400°C: 2.3	>85%	10	NA	NA	Repetition rate = 10 Hz; Fluence ~4 J/cm²

P_{O2}: oxygen gas pressure; d_{TS}: target-to-substrate distance; t: film thickness; RT: room temperature; NA: the data are not available.

Table 2. Summary of experimental conditions and properties of ITO films deposited with PLD using a 248 nm KrF excimer laser.

http://dx.doi.org/10.5772/65897

for films growth, and targets with different compositions can be sintered and used. In 1993, Zheng and Kwok [5] first reported the deposition of ITO by the pulsed laser ablation technique using an excimer laser at wavelength of 193 nm. The ITO target used was a 90 wt% In_2O_3 + 10 wt% SnO_2 sintered ceramic. The best electrical resistivity of the ITO films grown on glass substrate was 5.6×10^{-4} Ω cm and 1.4×10^{-4} Ω cm at substrate temperature of 20 and 310°C, respectively. The optical transmittance was greater than 90% for the optimized film between the wavelength ranges of 600 and 800 nm.

After the first successful deposition of ITO thin films on glass using the PLD technique was reported by Zheng and Kwok [5, 6], highly conductive ITO was deposited on InP substrates by PLD. The sample was then fabricated the ITO/p-InP device for the photovoltaic solar cell applications [7]. Thereafter, numerous studies on the ITO film initial growth and electrical conduction mechanism on different substrates using the same laser were reported [8–10]. When 248 nm KrF laser was used, ITO films with 85% optical transmittance in the visible and sheet resistance less than 1 Ω/sq were obtained at a substrate temperature of 200°C [11]. The properties of the ITO films were similar to the work done by using a 193 nm ArF laser. The properties of ITO films deposited at different conditions by using a KrF laser are summarized in **Table 2**.

An obvious disadvantage with excimer lasers is that its operation requires the handling of reactive gases. As an alternative, Nd:YAG solid-state laser has also been used for ITO deposition, especially after frequency doubled at 532 nm and frequency tripled at 355 nm. However, when the wavelength and pulse length are varied, it affects the laser penetration depth and the degree of absorption in laser-material interaction [3]. **Table 3** summarizes the experimental conditions and ITO thin films properties deposited by using an Nd:YAG pulsed laser at 355 and 532 nm in our previous reports as compared to others.

As a comparison, the effects due to the difference in laser wavelengths between 193 and 248 nm on the properties of the deposited ITO films are fairly small. A larger difference is observed for 193/248 nm deposition of ITO as compared to 355 nm deposition at room temperature. The resistivity that can be obtained by 193/248 nm laser is in the range of 10^{-4} Ω cm, while optimization in terms of ITO doping concentration [24] or substrate temperature [4, 26, 29] is needed in order to achieve the resistivity in the same range for 355 nm laser deposition.

Besides the need for sufficient Sn dopant in the ITO film, the deposition parameters: substrate temperature and background pressure are crucial to achieve the desired films properties. In the early reports, the resistivity of the films grown at lower substrate temperature was affected greatly by the background pressure as compared to those grown at higher temperature [5, 6]. The main reason for such an observation was ascribed to the film growth mechanisms in PLD. Upon ablation, the ablated plasma plume, consisting of Sn, In, and O species, undergoes collisions with the background gas that resultant in the final velocity distribution for each species. At higher substrate temperature, the low kinetic energy species will still be able to rearrange to form uniform films because of thermally induced migration from the heated substrate. Thus, deposition of high-quality films is possible covering a wider pressure range. However, at low substrate temperature, uniform films can only be obtained at an optimal velocity distribution which is affected greatly by the degree of collisions with the background gas. Thus, film

References	Substrate	ITO (wt.% of SnO_2)	Lowest resistivity	Optical transmittance	P_{O2} (mTorr)	d_{TS} (cm)	t nm)	Laser wavelength (nm)	Laser parameters
[22]	Glass	10	RT: 5×10^{-2} Ω cm 200°C: 1×10^{-3} Ω cm	RT: ~80% 200°C: ~90%	23	6	110	355	Pulsed duration = 6 ns; Repetition rate = 10 Hz; Fluence ~0.6 J/cm ^{2} *Deposition in various gas
[23]	Glass	10	RT: 1.1×10^{-3} Ω cm 200°C: 3.9×10^{-4} Ω cm	RT: >85% 200°C: >82%	23	6	110	355	Pulsed duration = 6 ns; Repetition rate = 10 Hz; Fluence ~2 J/cm^2
[24]	Glass	5	RT: 4.3×10^{-4} Ω cm200°C: 1.3×10^{-4} Ω cm	>80%	20	5	NA	355	Fluence ~2 J/cm^2
[25]	Silicon	In:Sn 9:1 alloy	RT: 500 Ω200°C: 80 Ω	NA	3750	3	NA	532	Fluence = 2 J/cm ^{2} Pulsed duration = 7 ns Repetition rate = 10 Hz
Our work [4, 26–28]	Glass PC	10	RT: 1×10^{-3} Ω cm 250°C: 3×10^{-4} Ω cm RT: 1.5×10^{-3} Ω cm	92% >85%	30	5	200	355	Fluence = 2.5 J/cm ^{2} Pulsed duration = 4.7 ns Repetition rate = 10 Hz
Our work [4, 26–28]	PC	10	RT: 3×10^{-3} Ω cm	>70%	30	5	200	532	Fluence = 2.5 J/cm ^{2} Pulsed duration = 4.7 ns Repetition rate = 10 Hz

Table 3. Summary of experimental conditions and properties of ITO films deposited with PLD using an Nd:YAG pulsed laser at 355 and 532 nm.

http://dx.doi.org/10.5772/65897

growth is rather sensitive to the background gas pressure. Similar trend has been observed in the deposition using excimer lasers [7, 13, 15] and the depositions using 355 nm laser [22, 30].

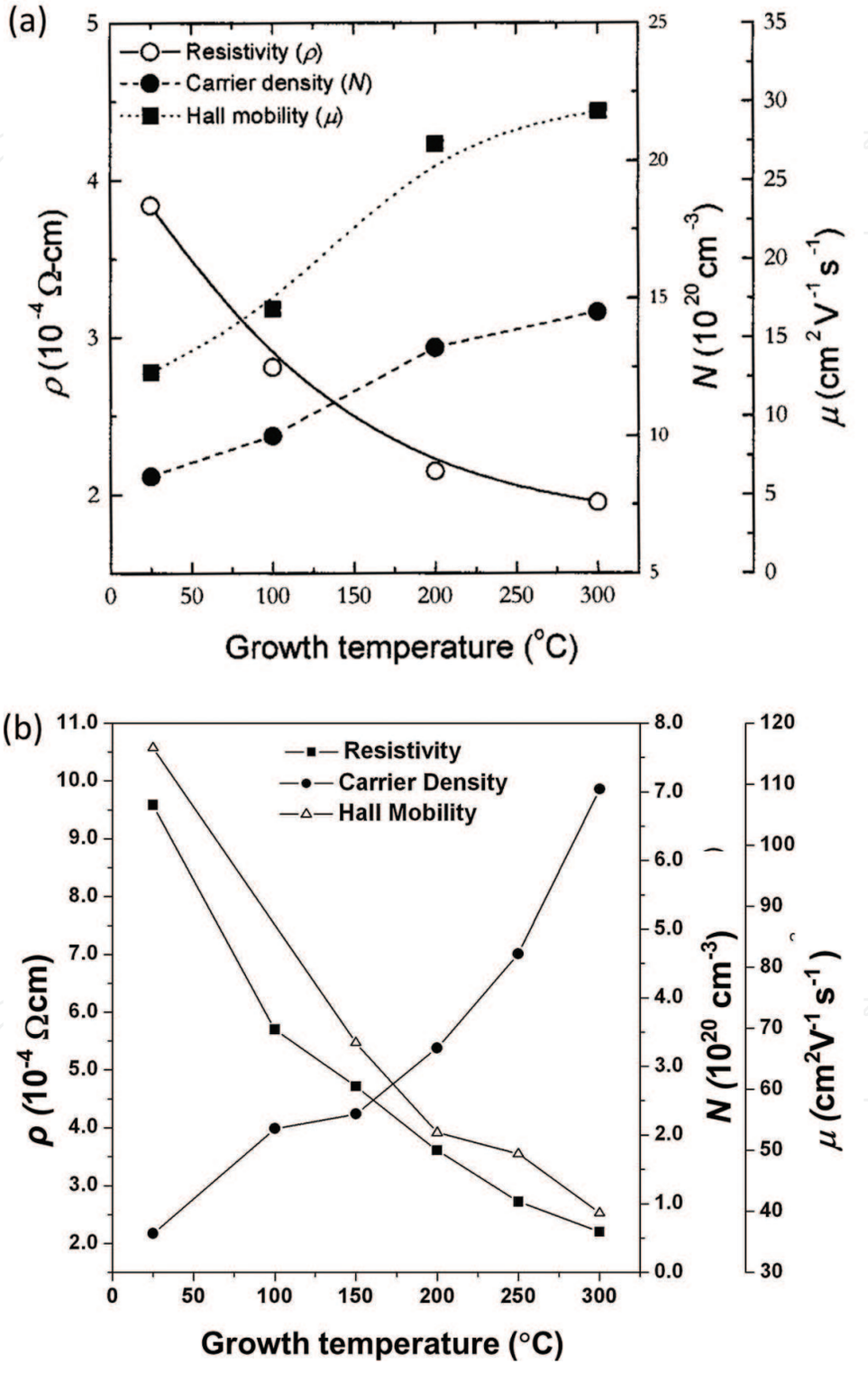

Figure 3. Effects of substrate temperature on film resistivity, carrier density, and Hall mobility deposited by (a) 248 nm laser at 10 mTorr [12] and (b) 355 nm laser at 30 mTorr [26].

http://dx.doi.org/10.5772/65897

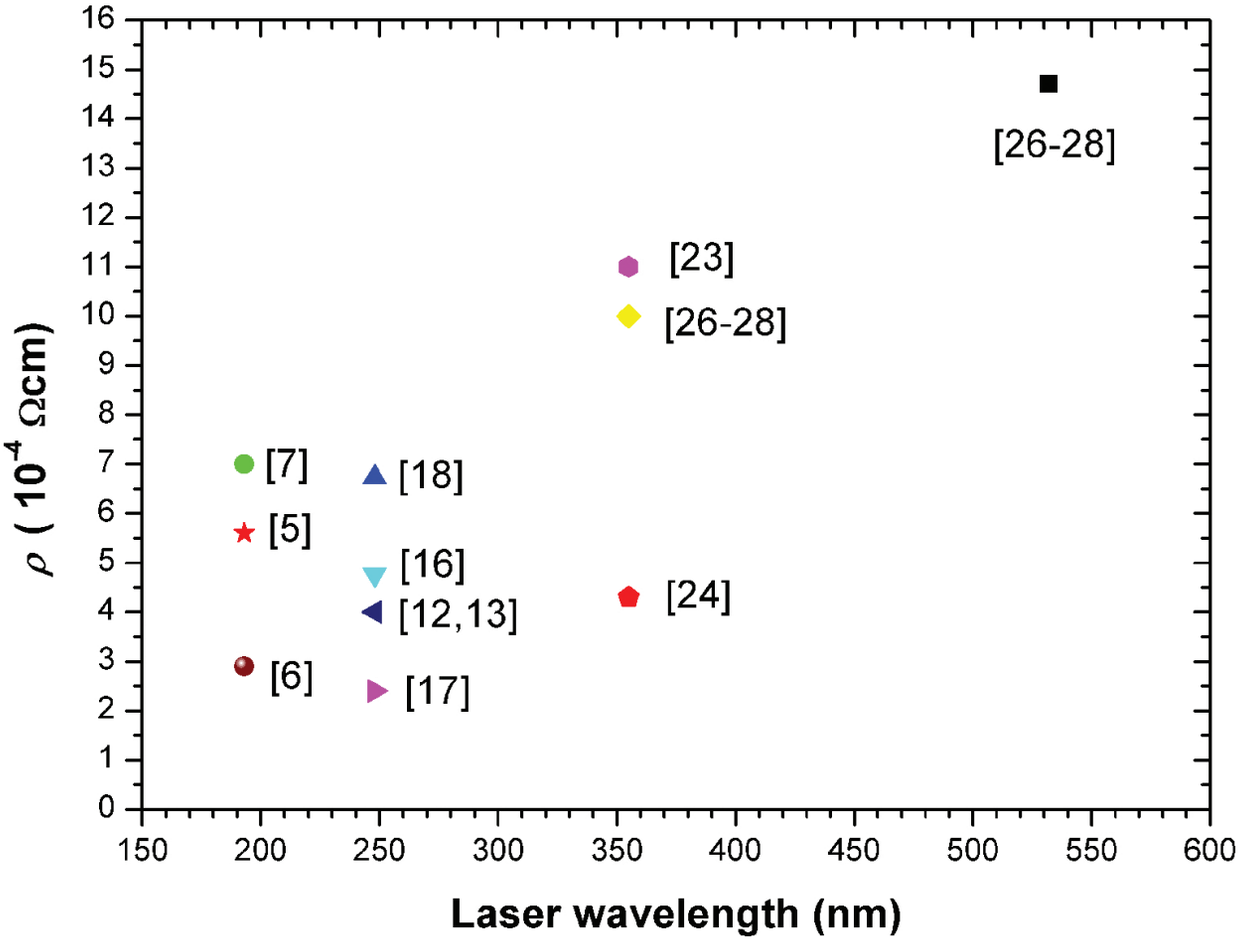

Figure 4. Resistivity of ITO films deposited in O_2 at RT as a function of laser wavelength.

In addition to the formation of a uniform film, substrate temperature affects the carrier density of the films and thus the resistivity of the ITO films. **Figure 3** shows the resistivity and the Hall effects measurement results of ITO films deposited by 248 nm [12] and a 355 nm laser [26]. As the substrate temperature was changed from room temperature (RT) to 300°C, the carrier density was doubled for the ITO films deposited by using 248 nm laser, while it was increased by 14 times for ITO deposited by using the 355 nm laser. At the same time, the Hall mobility was also increased by 2 times for ITO deposited by 248 nm laser, but the value was decreased by ~3 times for ITO deposited by 355 nm laser. Thus, effectively, the resistivity of ITO films in both cases was reduced at higher substrate temperature to ~2×10^{-4} Ω cm at 300°C. The results indicate that 248 nm laser was superior to 355 nm laser in the pristine deposition condition where the substrate was not heated, possibly due to the higher photon energy of 248 nm laser and its more congruent ablation with a smaller penetration depth [3]. Thus, ITO film properties that were inferior to those obtained by the shorter laser wavelengths were also obtained in 532 nm deposition [25, 28]. The resistivity of ITO films deposited at different laser wavelengths at RT is shown in **Figure 4**. However, substrate heating successfully improved the thin film property, and lower resistivity can be achieved for the case of 355 nm laser. The crystallinity of ITO films is also affected by substrate heating during the deposition process. The ITO films

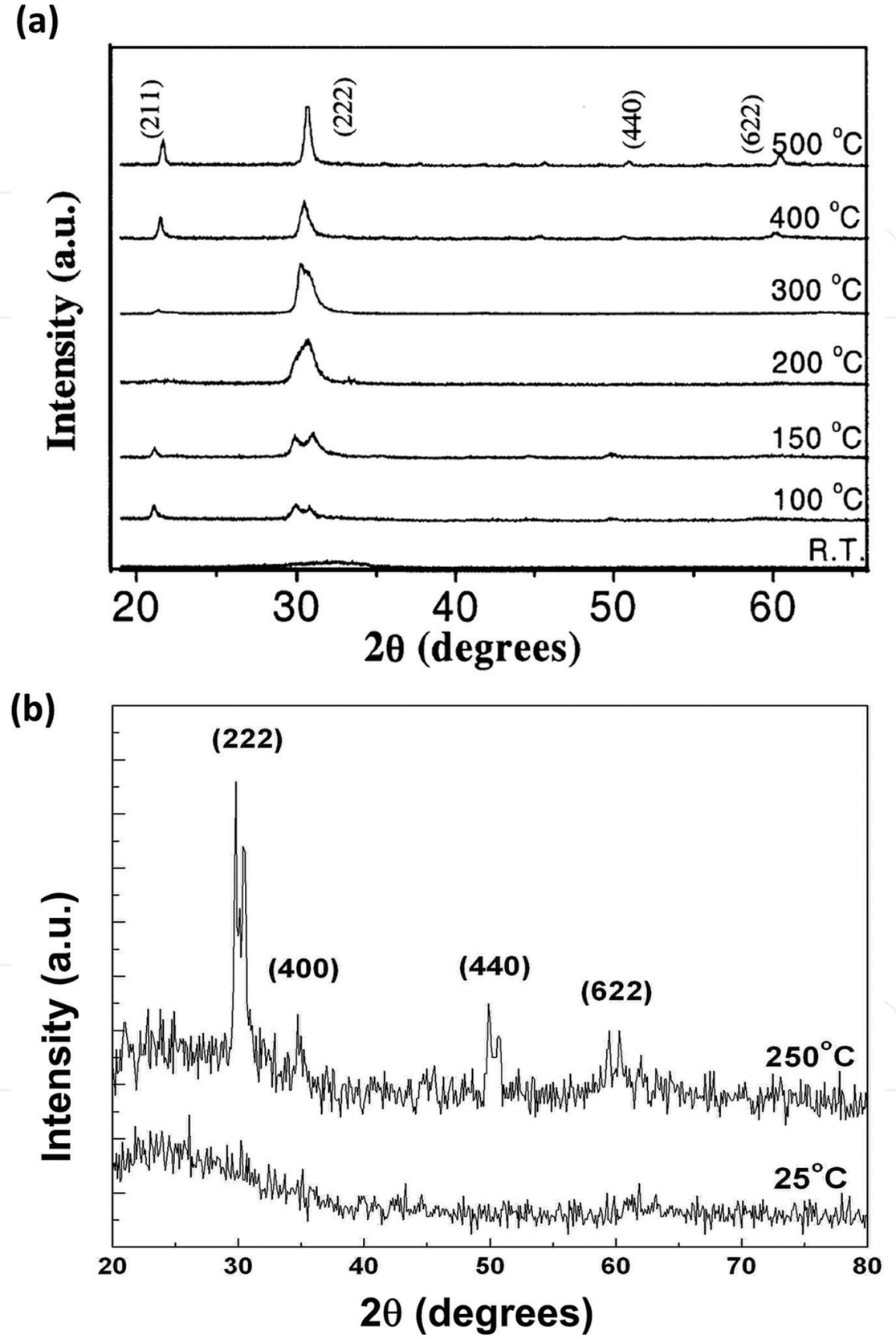

Figure 5. Effects of substrate temperature on the crystallinity of the ITO films deposited by (a) 248 nm laser [12] and (b) 355 nm laser [26].

are amorphous when deposited at RT by both 248 and 355 nm lasers. Crystalline films are obtained when deposited at above 100°C as shown in the XRD spectra in **Figure 5**.

ITO films deposited by laser ablation of ITO target have been applied in various applications such as solar cell [7, 31, 32], organic light-emitting devices [4, 12, 26], and more recently as low loss alternative plasmonic materials in the near-infrared region [33]. Our results show that ITO films with a range of properties can be obtained, controlled by the deposition parameters. PLD is capable of growing low resistivity, high transmittance ITO films at relatively low temperature or even room temperature that are beneficial for device application onto delicate polymer substrates or active materials.

3. Pulsed laser deposition of ITO nanostructures.

The growth of ITO nanostructures (nanowires, nanorods, nanowhiskers, and nanocrystals) is desirable because of the distinct nanoscale effects in addition to the advantages in large contact areas offered by nanomaterials. The nanoeffects of ITO nanostructures have been demonstrated in various aspects based on the UV light-emitting properties [34], terahertz and far-infrared transmitting characteristics [35], and field emission properties [36]. PLD, as a flexible and versatile tool for materials deposition, was first shown to be capable for the growth of nanowires by using excimer laser ablation in 2006 [37]. ITO nanowires were grown on catalyst-free oxidized silicon substrates at 500°C in nitrogen atmosphere. The growth of nanostructures was not observed by others although the growth involving non-oxygen gases such as N_2 [19], rare gas Ne, Ar, and Xe [22] (**Tables 2** and **3**) has been reported. In this report, ITO films with lower resistivity and higher transmittance were obtained when deposited in O_2. However, in the report by Savu and Joanni [37], when higher substrate temperate and Si substrate were used, nanostructural growth of ITO was observed in N_2. The morphology of the nanostructures was found to be highly dependent on the N_2 gas pressure as shown in

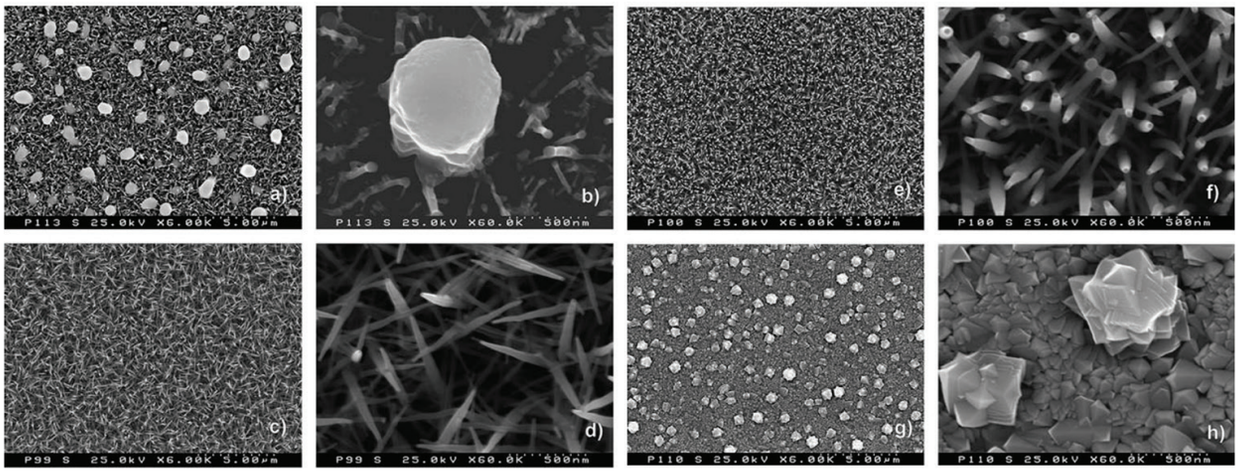

Figure 6. Surface images of nanostructured films deposited at 0.1 mbar (a, b), 0.5 mbar (c, d), 1 mbar (e, f), and 2 mbar (g, h) [37].

Figure 6. The growth mechanisms were proposed to be related to vapor-liquid-solid growth as a large amount of liquid was formed, especially at low pressure, thus promoting the growth of thin, branched nanowires. As the deposition pressure increases, the amount of liquid phase decreases, resulting in formation of nanowires having fewer branches. At a pressure of 1 mbar, the wires were almost perpendicular to the substrate and free of branches. At 2 mbar, columnar dense film is formed with large pyramidal and triangular structures.

Based on a standard PLD setup as shown in **Figure 2**, we studied the effects of different background gases Ar, He, N_2, and O_2 in details [38–40]. Glass substrates were used, and the growth was performed at a lower substrate temperature of 250°C. ITO nanostructures were formed, and the morphology of the nanostructures formed in different gases is shown in **Figure 7** [40]. The ITO film was uniform in size when deposited in O_2, while ITO deposited in Ar consisted of ultrafine nano-grains with a size of < 50 nm. For ITO deposited in N_2, the nanostructure consisted of porous network of nanorods of about 30 nm in diameter and 300 nm in length. Larger structures were obtained when deposited in He. ITO nanostructures formed in Ar, He, and O_2 were highly crystalline and possess higher transmittance than those obtained in N_2. The resistivity for ITO nanostructures deposited in N_2 was also higher than those deposited in Ar, He, and O_2. The results show that nanostructures can be obtained under specific conditions, which is not limited to higher temperature range and Si substrates in the first report by Savu and Joanni [37].

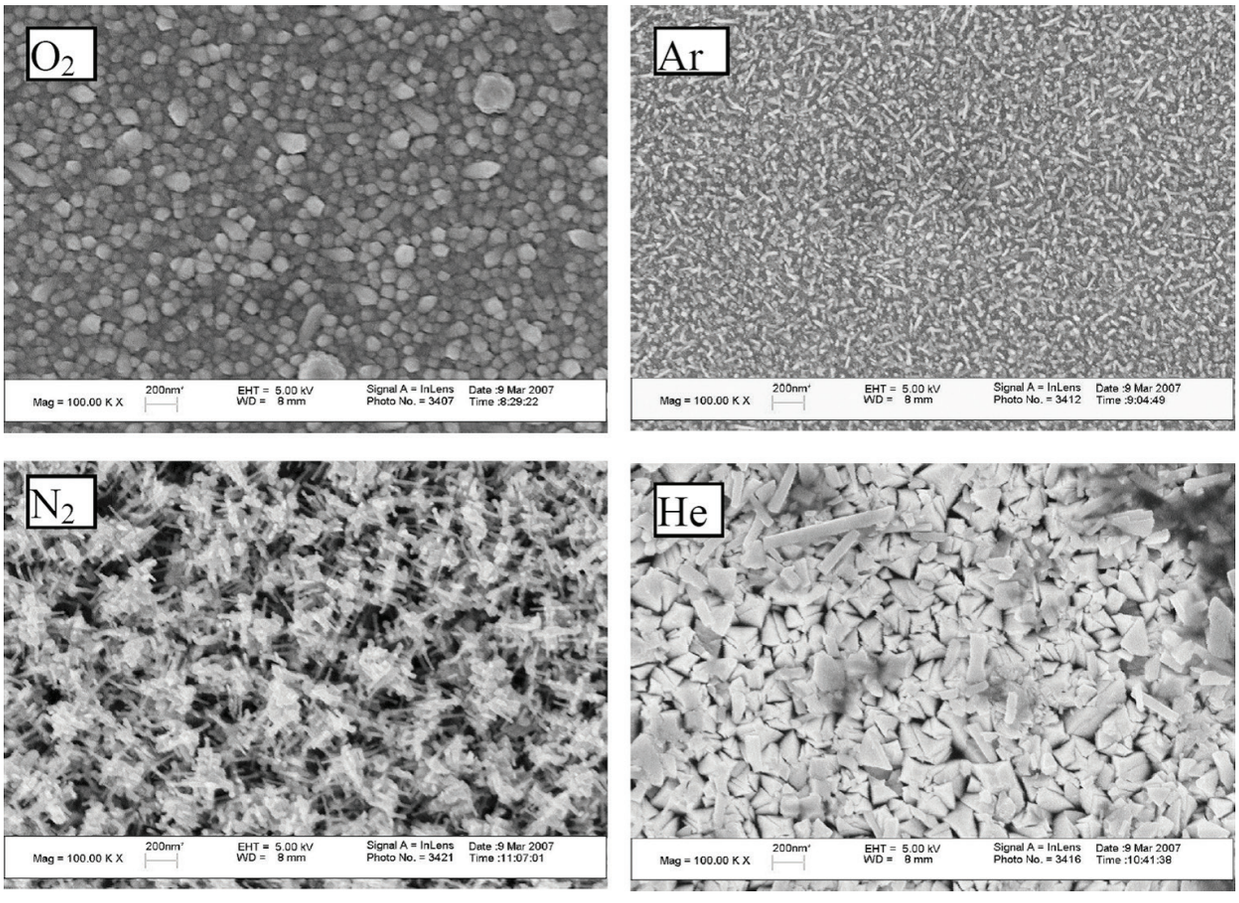

Figure 7. Effects of the background gas on the ITO microstructures. (a) O_2, (b) Ar, (c) N_2, and (d) He [40].

http://dx.doi.org/10.5772/65897

Further studies were performed for the growth in He and Ar at different background pressures based on the same setup [39]. The pressure range was chosen by considering the molecular

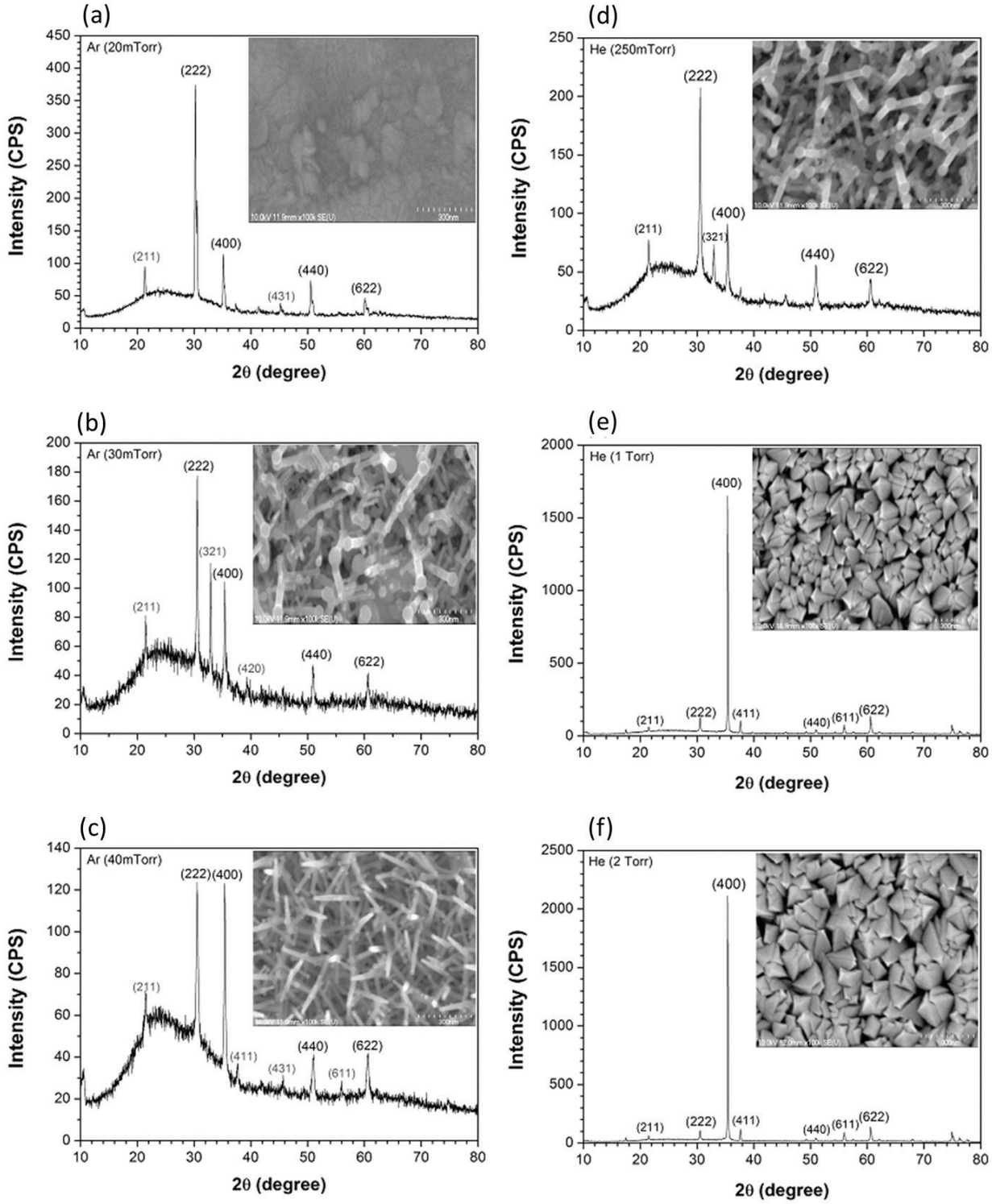

Figure 8. XRD and SEM of ITO samples grown in Ar ambient at (a) 20 mTorr, (b) 30 mTorr, and (c) 40 mTorr and grown in He at (d) 250 mTorr, (e) 1 Torr, and (f) 2 Torr [39].

ITO samples	Resistivity ($\times 10^{-4}\Omega$ cm)	Carrier density ($\times 10^{20}$ cm^{-3})	Hall mobility (cm^2/Vs)
Commercial ITO	1.97	18.7	16.6
Ar (30 mTorr, 250°C)	1.61	10.5	36.7
Ar (40 mTorr, 250°C)	2.09	6.65	44.9
He (250 mTorr, 250°C)	9.37	13.2	5.06
He (1000 mTorr, 250°C)	1.91	6.91	4.75
He (2000 mTorr, 250°C)	7.75	9.50	8.78

Table 4. Resistivity, carrier density, and Hall mobility of commercial ITO and ITO samples grown in Ar and He ambient.

weight of the gas that will affect the collision with ablated species. The growth was performed by PLD using a 355 nm laser at a substrate temperature of 250°C. The results show that nanostructures growth was dependent critically on the background pressure (**Figure 8**), similar to those reported in N_2 [37]. ITO nanowires were obtained in both gases. For ITO deposited in Ar, XRD diffraction patterns corresponding to (222), (400), (440), and (622) orientations of cubic bixbyite structure of ITO were detected. As the pressure of Ar increased, the (400) diffraction peak became relatively stronger, indicating the increase in crystalline orientation.

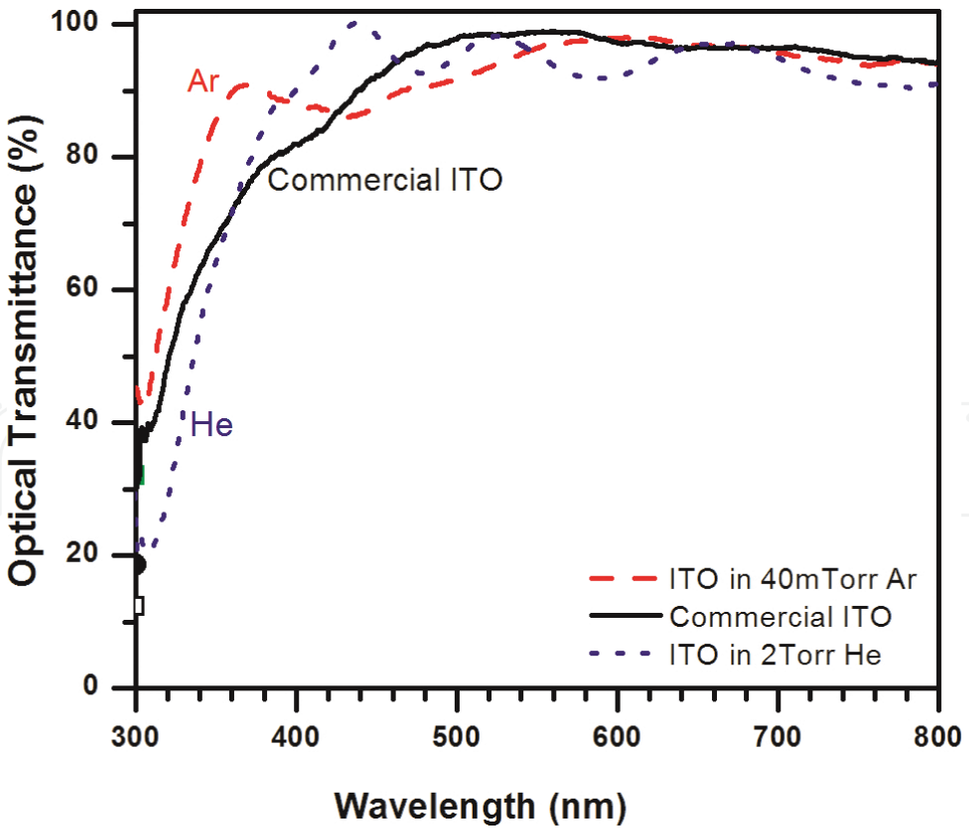

Figure 9. Optical transmittance of commercial ITO and ITO samples grown in Ar and He background gases [39].

At 30 mTorr, ITO nanowires were formed, and some spherical particles were observed on their tips, which suggest that they are formed by the vapor-liquid-solid (VLS) mechanism. At higher pressure of 40 mTorr, nanowires with smaller diameters were observed. No spherical particles were observed, and the tips were sharp, unlike those obtained at lower pressure. When deposited in He, nanowires were obtained at 250 mTorr, and spherical tips were formed on the tips. As the pressure increased, larger pyramid shape crystals were obtained, and the crystals orientation are aligned to (400). Both nanostructures grown in Ar and He exhibited good resistivity in the range of 10^{-4} Ω cm, and nanowires grown in Ar exhibited even higher carrier mobility than those measured from a commercial ITO sample. The values are shown in **Table 4**. **Figure 9** shows the optical transmittance of ITO nanostructures grown in Ar and He as compared to a commercial ITO sample. In addition, ITO nanowires grown by PLD are tested as TCO layer for a standard OLED device. ITO nanowires with larger contact areas and higher charge injection have led to higher emission current density for the devices [39].

4. Conclusion

Laser ablation of ITO target was studied in various aspects. Pulsed laser ablations by 193, 248, or 355 nm lasers in low vacuum conditions afforded the deposition of high-quality ITO films at relatively low temperatures. This was largely ascribed to the production of homogenous, energetic, and atomized plasma plume. The effects of substrate temperature, background gas pressure, in particular the O_2 on the electrical and optical properties of ITO films have been presented and discussed. In addition to the normal consensus that ITO depositions are to be performed in O_2 to preserve the stoichiometry of the final films, pulsed laser ablation of ITO target, when performed in various gases such as Ar, He, or N_2, could promote the growth of ITO nanostructures. At optimized pressure, the gas-phase condensation successfully induced nucleation and growth of the nanostructures such as nanorods and nanowires on glass substrate at relatively low substrate temperature.

Acknowledgements

We acknowledge the financial support from Penang State Government, Telekom Malaysia, the Ministry of Science, Technology and Innovation, and the Ministry of Higher Education of Malaysia in the form of research grants.

Author details

Seong Shan Yap[1,*], Thian Khok Yong[2], Chen Hon Nee[1] and Teck Yong Tou[1]

*Address all correspondence to: seongshan@gmail.com

1 Faculty of Engineering, Multimedia University, Cyberjaya, Selangor, Malaysia

2 Lee Kong Chian Faculty of Engineering and Science, Universiti Tunku Abdul Rahman, Bandar Sungai Long, Kajang, Selangor, Malaysia

References

[1] Ellmer K. 2012. Past achievements and future challenges in the development of optically transparent electrodes. Nat. Photon. 6:809–17

[2] Hamberg I, Granqvist C G, Berggren K-F, Sernelius B E and Engström L. 1984. Band-gap widening in heavily Sn-doped In_2O_3. Phys. Rev. B 30:3240–9

[3] Chrisey D B and Hubler G K. editors. Pulsed Laser Deposition of Thin Films. Wiley; 1994. 648 p. ISBN 0471592188/9780471592181.

[4] Yong T K, Yap S S, Sáfrán G and Tou T Y. 2007. Pulsed Nd:YAG laser depositions of ITO and DLC films for OLED applications. Appl. Surf. Sci. 253:4955–9

[5] Zheng J P and Kwok H S. 1993. Low resistivity indium tin oxide films by pulsed laser deposition. Appl. Phys. Lett. 63:1–3

[6] Zheng J P and Kwok H S. 1993. Preparation of indium tin oxide films at room temperature by pulsed laser deposition. Thin Solid Films. 232:99–104

[7] Jia Q X, Zheng J P, Kwok H S and Anderson W A. 1995. Indium tin oxide on InP by pulsed-laser deposition. Thin Solid Films. 258:260–3

[8] Sun X W, Huang H C and Kwok H S. 1996. In-situ resistance measurements during pulsed laser deposition of ultrathin films. Appl. Surf. Sci. 106:51–4

[9] Sun X W, Kim D H and Kwok H S. 1998. Ultra thin indium tin oxide films on various substrates by pulsed laser deposition Mater. Res. Soc. Symp. Proc. 485:267–72

[10] Sun X W, Huang H C and Kwok H S. 1996. On the initial growth of indium tin oxide on glass. Appl. Phys. Lett. 68:2663–5

[11] Hanus F, Jadin A and Laude L D. 1996. Pulsed laser deposition of high quality ITO thin films. Appl. Surf. Sci. 96–98:807–10

[12] Kim H, Gilmore C M, Piqué A, Horwitz J S, Mattoussi H, Murata H, Kafafi Z H and Chrisey D B. 1999. Electrical, optical, and structural properties of indium-tin-oxide thin films for organic light-emitting devices. J. Appl. Phys. 86:6451–61

[13] Kim H, Horwitz J S, Piqué A, Gilmore C M and Chrisey D B. 1999. Electrical and optical properties of indium tin oxide thin films grown by pulsed laser deposition. Appl. Phys. A Mater. Sci. Process. 69:S447–50

[14] Kim H, Horwitz J S, Kushto G P, Kafafi Z H and Chrisey D B. 2001. Indium tin oxide thin films grown on flexible plastic substrates by pulsed-laser deposition for organic light-emitting diodes. Appl. Phys. Lett. 79:284–6

[15] Adurodija F O, Izumi H, Ishihara T, Yoshioka H, Yamada K, Matsui H and Motoyama M. 1999. Highly conducting indium tin oxide (ITO) thin films deposited by pulsed laser ablation. Thin Solid Films. 350:79–84

[16] Adurodija F O, Izumi H, Ishihara T, Yoshioka H and Motoyama M. 2002. The electro-optical properties of amorphous indium tin oxide films prepared at room temperature by pulsed laser deposition. Sol. Energy Mater. Sol. Cells 71:1–8

[17] Izumi H, Ishihara T, Yoshioka H and Motoyama M. 2002. Electrical properties of crystalline ITO films prepared at room temperature by pulsed laser deposition on plastic substrates. Thin Solid Films. 411:32–5

[18] Craciun V, Craciun D, Chen Z, Hwang J and Singh R K. 2000. Room temperature growth of indium tin oxide thin films by ultraviolet-assisted pulsed laser deposition. Appl. Surf. Sci. 168:118–22

[19] Morales-Paliza M, Huang M and Feldman L. 2003. Nitrogen as background gas in pulsed-laser deposition growth of indium tin oxide films at room temperature. Thin Solid Films. 429:220–4

[20] Kim S H, Park N M, Kim T and Sung G. 2005. Electrical and optical characteristics of ITO films by pulsed laser deposition using a 10 wt.% SnO_2-doped In_2O_3 ceramic target. Thin Solid Films. 475:262–6

[21] Petukhov I A, Shatokhin A N, Putilin F N, Rumyantseva M N, Kozlovskii V F, Gaskov A M, Zuev D A, Lotin A A, Novodvorsky O A and Khramova A. D. 2012. Pulsed laser deposition of conductive indium tin oxide thin films. Inorg. Mater. 48:1020–5

[22] Thestrup B, Schou J, Nordskov A and Larsen N B. 1999. Electrical and optical properties of thin indium tin oxide films produced by pulsed laser ablation in oxygen or rare gas atmospheres. Appl. Surf. Sci. 142:248–52

[23] Thestrup B and Schou J. 1999. Transparent conducting AZO and ITO films produced by pulsed laser ablation at 355 nm. Appl. Phys. A 69:807–10

[24] Choi J B, Kim J H, Jeon K A and Lee S Y. 2003. Properties of ITO films on glass fabricated by pulsed laser deposition. Mater. Sci. Eng. B 102:376–9

[25] Teghil R, Marotta V, Guidoni A G, Di Palma T M and Flamini C. 1999. Reactive pulsed laser ablation and deposition of thin indium tin oxide films for solid state compact sensors. Appl. Surf. Sci. 138 522–6

[26] Yong T-K, Yap S-S and Tou T-Y. 2008. Parametric studies of pulsed Nd:YAG laser deposition of ITO for OLED application. Rev. Laser Eng. 36:1242–5

[27] Yong T-K, Kee Y-Y, Tan S-S, Yap S-S, Siew W-O and Tou T-Y. 2010. The effects of sodium in ITO by pulsed laser deposition on organic light-emitting diodes. Appl. Phys. A 101:621–6

[28] Yong T K, Tou T Y and Teo B S. 2005. Pulsed laser deposition of tin-doped indium oxide (ITO) on polycarbonate. Appl. Surf. Sci. 248:388–91

[29] Holmelund E, Thestrup B, Schou J, Larsen N B, Nielsen M M, Johnson E and Tougaard S. 2002. Deposition and characterization of ITO films produced by laser ablation at 355 nm. Appl. Phys. A: Mater. Sci. Process. 74:147–52

[30] Tou T-Y, Yong T-K, Yap S-S, Yang R-B, Siew W-O and Yow H-K. 2009. Parametric studies of pulsed laser deposition of indium tin oxide and ultra-thin diamond-like carbon for organic light-emitting devices. J. Opt. Soc. Korea 13:65–74

[31] Trehame R E, Seymour-Pierce A, Durose K, Hutchings K, Roncallo S and Lane D. 2011. Optical design and fabrication of fully sputtered CdTe/CdS solar cells. J. Phys. Conf. Ser. 286:12038

[32] Wu C, Zhang Z, Wu Y, Lv P, Nie B, Luo L, Wang L, Hu J and Jie J. 2013. Flexible CuS nanotubes-ITO film Schottky junction solar cells with enhanced light harvesting by using an Ag mirror. Nanotechnology 24:45402

[33] Fang X, Mak C L, Zhang S, Wang Z, Yuan W and Ye H. 2016. Pulsed laser deposited indium tin oxides as alternatives to noble metals in the near-infrared region. J. Phys. Condens. Matter 28:224009

[34] Gao J, Chen R, Li D H, Jiang L, Ye J C, Ma X C, Chen X D, Xiong Q H, Sun H D and Wu T. 2011. UV light emitting transparent conducting tin-doped indium oxide (ITO) nanowires. Nanotechnology 22:195706

[35] Yang C, Chang C, Chen P, Yu P and Pan C-L. 2013. Broadband terahertz conductivity and optical transmission of indium-tin-oxide (ITO) nanomaterials. Opt. Express 21:16670–82

[36] Wan Q, Feng P and Wang T H. 2006. Vertically aligned tin-doped indium oxide nanowire arrays: epitaxial growth and electron field emission properties. Appl. Phys. Lett. 89:3–5

[37] Savu R and Joanni E. 2006. Low-temperature, self-nucleated growth of indium-tin oxide nanostructures by pulsed laser deposition on amorphous substrates. Scr. Mater. 55:979–81

[38] Yong T-K, Tan S-S, Nee C-H, Yap S-S, Kee Y-Y, Sáfrán G, Horváth Z E, Moscatello J, Yap Y-K and Tou T-Y. 2012. Pulsed laser deposition of indium tin oxide nanowires in argon and helium. Mater. Lett. 66:280–1

[39] Kee Y Y, Tan S S, Yong T K, Nee C H, Yap S S, Tou T Y, Sáfrán G, Horváth Z E, Moscatello J P and Yap Y K. 2012. Low-temperature synthesis of indium tin oxide nanowires as the transparent electrodes for organic light emitting devices. Nanotechnology 23:25706

[40] Yong T K, Nee C H, Yap S S, Siew W O, Sáfran G, Yap Y K and Tou T Y. 2010. Pulsed laser deposition of nanostructured indium-tin-oxide film. In R J Martin-Palma, Y-J Jen and A Lakhtakia (eds) Proceedings of the SPIE, vol. 7766, pp 776615–6